Polymer Chemistry

ROYAL SOCIETY OF CHEMISTRY

PAPER

View Article Online
View Journal

Cite this: DOI: 10.1039/d5py00334b

Microfluidic-supported emulsion polymerization: molecular weight and concentration of surface-capping agents impact the formation of anisotropic polyvinylmethacrylate particles

Nikunjkumar R. Visaveliya, †[a] Seda Kelestemur,†[a,b] Firdaus Khatoon,[a] Jin Xu,[a] Kelvin Leo,[a] Karisma McCoy,[a] Lauren St. Peter,[a] Christopher Chan,[a] Tatiana Mikhailova,[a] Visar Bexheti,[a] Geri Shentolli,[a] Anushan Alagaratnam,[a] Saad Ahmed,[a] Piyali Maity[a] and Dorthe M. Eisele *[a,c]

Surface-capping agents—for example, amphiphilic surfactant molecules, water-soluble polymers, or polyelectrolytes—play a critical role during polymerization reactions for both the formation and stability of colloidal polymer particles. Here, we investigated the effect of the molecular weight and concentration of polymeric surface-capping agents on the assembling of polyvinyl methacrylate (PVMA) colloidal nanoparticles (NPs) *via* microfluidic-supported emulsion polymerization. Specifically, the impacts of the molecular weight and concentration of polyvinylpyrrolidone (PVP, molecular weights of 10 000, 40 000, 360 000, and 1 300 000 MW, concentrations of 0.05, 0.5, 1, 2.5, 5, and 10 mM, repeating unit concentration) and poly(sodium styrene sulfonate) (PSSS, molecular weights of 70 000 and 200 000 MW, concentrations of 0.1, 1, 2.5, 5, 10, and 20 mM, repeating unit concentration) on the formation of PVMA NPs were investigated. Depending on the molecular weight and concentration of surface-capping agents, we obtained finely textured assembled, spherical, flower-shaped, fluffy, and elongated spherical PVMA NPs with sizes ranging from 70 to 500 nm. With our microfluidic-supported synthesis of PVMA NPs, we contributed to a basic understanding of how the molecular weight and concentration of surface-capping agents impact the formation of polymer NPs.

Received 3rd April 2025,
Accepted 21st April 2025

DOI: 10.1039/d5py00334b

rsc.li/polymers

1. Introduction

Colloidal polymer particles[1–7] are widely used in several applications such as targeted drug delivery,[8–10] tissue engineering,[11] surface coating,[12] and medical imaging.[13,14] The interior and surface properties of colloidal polymer particles play a crucial role during interaction with active surfaces of biological and non-biological materials.[15–23] In particular, the surface properties of colloidal polymer particles can be controlled post-synthetically *via* various techniques such as soft lithographic techniques or solvent evaporation processes.[24–27] However, the time-consuming post-synthetic treatments do not meet the requirements to control the size and shape of polymeric particles. Therefore, easy and rapid *in situ* routes for controlling the structural surface properties of polymeric colloids are in high demand.

Emulsion polymerization is a versatile method to obtain colloidal particles with tunable sizes.[28–31] Molecular surfactants stabilize the surface of nanoparticles and simultaneously control the growth of particles in solution during polymerization.[32–34] Molecular surfactants, such as anionic sodium dodecyl sulfate (SDS) and cationic cetyltrimethylammonium bromide (CTAB), can form spherical micellar structures above their critical micelle concentration (CMC).[35] Surface-capping agents can also protect colloidal particles against uncontrolled aggregation.[33,34] On the other hand, a polymeric surface-capping agent can act as a dynamic surface-controlling agent to initiate the assembling process of particles.[32,36] Under controlled conditions, colloidal particles can create diverse structures from the nano- to sub-micron length scale that find use in a myriad of rheological and interfacial applications.[37–41] When soft polymer nanoparticles assemble during polymerization in a controlled manner, a wide range of anisotropic shapes can be generated.[42,43]

[a]*Department of Chemistry and Biochemistry, The City College of New York at The City University of New York, New York, NY, USA. E-mail: eisele@eiselegroup.com*
[b]*Biotechnology Department, Institute of Health Sciences, University of Health Sciences, Istanbul, Turkey*
[c]*Ph.D. Program in Chemistry, Graduate Center of The City University of New York, New York, NY, USA*
†These authors contributed equally.

Compared to their spherical counterparts, anisotropic polymer nanoparticles are of particular importance due to their higher surface area (at the same length scale), making them suitable candidates for various medical applications.[44,45]

The importance of the molecular weight and concentration of surface-capping agents on particle shape and size was demonstrated in earlier studies.[46–48] Previously, the role of polymeric surface-capping agents in the generation of shape-tunable polymethyl methacrylate (PMMA) nanoparticles has been investigated in detail.[30,42,43] In addition, recently, the impacts of five different types of surface-capping agents on the formation of colloidal polyvinyl methacrylate (PVMA) particles —employing the monomer unit with dual polymerization active sites—have been investigated.[49] In our previous work,[49] it was found that different types of surface-controlling agents have different roles in the formation of PVMA colloidal particles. Specifically, we showed that both the monomer type and interfacial agent play a role in controlling the anisotropic assembling pattern of colloidal PVMA NPs.[49] Vinyl methacrylate (VMA) is a non-viscous monomer suitable for several polymerization methods, for example, nitroxide-mediated polymerization. Nitroxide-mediated polymerization, a controlled radical polymerization, is generally used for styrene and acrylate-based monomers without any bulky group (including methyl) attached to their double bonds.[50,51] In addition, VMA monomers and their derivatives also impact the reversible-addition–fragmentation chain-transfer (RAFT) polymerization.[52,53]

In this work, we studied the impact of the molecular weight and concentration of mainly two different types of polymeric surface-capping agents (polymer polyvinyl pyrrolidone (PVP) and polyelectrolyte poly(styrene sulfonate sodium salt) (PSSS)) on the growth and *in situ* assembly of PVMA colloidal particles *via* microfluidic-supported polymerization. We used non-ionic PVP with four different molecular weights (10 000, 40 000, 360 000, and 1 300 000 MW, concentrations of 0.05, 0.5, 1, 2.5, 5, and 10 mM, repeating unit concentration) and an anionic PSSS with two different molecular weights (70 000 and 200 000 MW, concentrations of 0.1, 1, 2.5, 5, 10, and 20 mM, repeating unit concentration) in the aqueous phase. We demonstrated that the assembling processes of colloidal PVMA particles can be controlled based on tunable molecular weights and concentrations of the surface-capping agents. Finely textured assembled, spherical, flower-shaped, fluffy, and elongated spherical PVMA NPs were obtained using PVP and PSSS. Utilization of a microfluidic platform[54–57] is a very efficient approach for providing uniform reaction mixing conditions. In our study, we used a cross-flow-based microfluidic reactor[35] for the emulsification of two immiscible liquid phases. The polymerization of the emulsified solution was performed externally as shown in Fig. 1 (semi-microfluidic process).

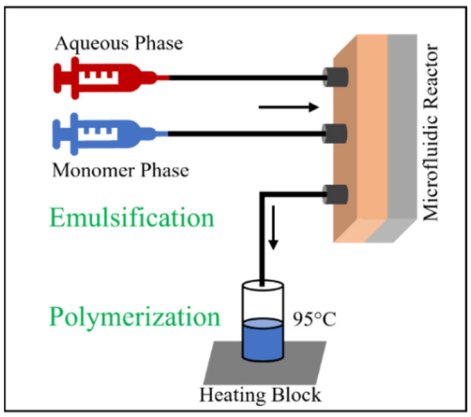

Fig. 1 Experimental setup. The schematic illustrates the microfluidic-supported (semi-microfluidic) setup for the polymerization process in which emulsification of both immiscible liquid phases takes place in a microfluidic reactor and completion of the polymerization takes place at the heating block.

2. Results and discussion

The impact of PVA and PSSS with different molecular weights on the formation of PVMA colloidal particles was identified through the *in situ* assembling of colloids in the aqueous phase. All molecular weights of the polymeric surface-controlling agents (PVP and PSSS) are considered in grams per mole, and their concentration has been calculated based on their repeating unit concentration. Thermal polymerization was conducted by using a thermal initiator, azobisisobutyronitrile (AIBN) which was dissolved in the monomer phase including VMA and ethylene glycol dimethacrylate (EGDMA) (Fig. 2).

2.1 Colloidal PVMA particles: impact of tunable molecular weights and concentrations of PVP

Here, the impact of non-ionic PVP with various molecular weights and concentrations on the formation of PVMA NPs was investigated. In general, during the emulsion polymerization, the interaction between the monomer droplets and PVP results in the formation of PVMA NPs. Initially, an emulsion of the VMA-contained monomer phase and PVP-contained

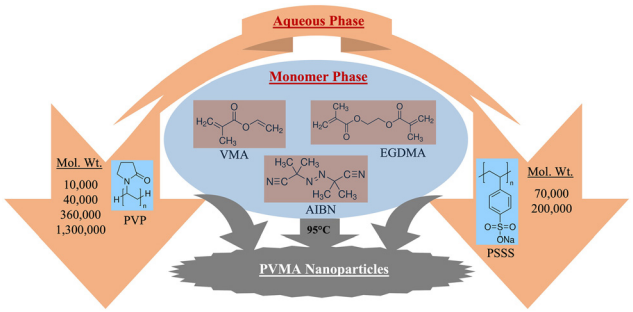

Fig. 2 Schematic illustration providing an overview of the polymerization for the synthesis of PVMA NPs. The aqueous phase is made up from polymeric surface-capping agents of variable molecular weights and the monomer phase is a mixture of the monomer, cross-linker, and thermal initiator. Polymerization was conducted at 95 °C for the formation of PVMA colloidal particles.

aqueous phase is generated in the microfluidic reactor, as shown in Fig. 1. When the nucleation stage of the polymerization begins, the formation of small-sized nanoparticles (early growth state) is followed by continuous growth.[58] PVP, as a surface-capping agent, gets attached to the surface of growing colloidal NPs and controls the growth dynamics of the NPs. When water-soluble polymers are used, such as PVP, the control of the surface properties of the growing NPs is driven by steric stabilization.[29]

The aggregation mechanism for the growth of PVMA NPs is comparable with the mechanism of PMMA NPs, as described previously.[30] In contrast to PMMA NP synthesis, however, we obtained morphologically different PVMA NPs at various concentrations of PVP of tunable molecular weights. PVP controls the solvation and mobility of the growing PVMA NPs during the polymerization reaction. When particles are small (early growth stage), their solvation and mobility in an aqueous solution are high but when the particles' size is at the threshold level, they assemble (aggregate) to reduce their surface energy.[59] Depending on the concentration and molecular weight of PVP, we obtained finely textured assembled, flower-shaped, and spherical PVMA NPs. Flower-shaped PVMA particles were obtained as a result of multi-step assembling processes at certain concentrations.[30]

2.1.1. Utilizing PVP-10 000 (molecular weight) in the aqueous phase. PVP-10 000 (concentrations of 0.5, 1, 5, and 10 mM, repeating unit concentration) was used to obtain PVMA NPs. 180 nm diameter finely textured surface PVMA NPs were formed using 10 mM PVMA as depicted in Fig. 3A. With the decrease of the PVP concentration down to 5 mM in the aqueous phase, no significant change in the obtained NPs was observed compared to using 10 mM PVP. In the case of using 5 mM PVP, the finely textured surface PVMA colloidal particles were obtained with a slightly smaller size with a diameter of about 140 nm as shown in Fig. 3B. Furthermore, the assembling pattern formed flower-shaped PVMA colloidal particles when the PVP concentration was decreased to 1 mM repeating unit concentration (Fig. 3C). According to our final products, we can conclude that the enhanced texture of the surface of PVMA colloidal particles was formed due to the increased polymerization rate at a lower PVP concentration. The number of formed PVMA particles is less at a low PVP concentration and the polymerization rate is faster because the surface is slightly covered with a surface-capping agent (PVP). When polymerization is faster, the particles grow quickly before they achieve the aggregation stage and the aggregation is observed during the later phases of polymerization.[60] Indeed, larger PVMA aggregates and flower-shaped PVMA NPs were obtained at 1 mM concentration. With the further decrease of the PVP concentration to 0.5 mM, spherical-shaped particles were obtained (Fig. 3D). The final size of the spherical PVMA particles is smaller (less than 150 nm, Fig. 3D) compared to the flower-shaped particles (Fig. 3C). According to our final products, it can be assumed that the particles with textured surfaces as shown in Fig. 3A–C are likely the result of aggregation of smaller-sized spherical NPs whereas the particles with smooth surfaces as shown in Fig. 3D are individual particles formed without aggregation. The measured zeta potential of the PVP-covered PVMA colloidal particles is around −17 mV at all concentrations as shown in Fig. 3E. The negative value of the zeta potential of PVMA colloidal particles may be a result of the enolization of the PVP in the aqueous phase as well as the radicals generated by the initiator AIBN.[61,62]

2.1.2 Utilizing PVP-40 000 (molecular weight) in the aqueous phase. Large clustered and randomly aggregated PVMA NPs were obtained by using a 10 mM repeating unit concentration of PVP-40 000 as shown in Fig. 4A. The observed surface textures of PVMA NPs that were obtained *via* using PVP at the same concentrations of 10 000 and 40 000 molecular weights are very different, as shown in Fig. 3A and 4A, respectively. Also, the flower-shaped PMMA NPs with enhanced surface textures were obtained using different molecular weights of PVP from those previously used for PVMA NPs.[30] This finding suggests that alongside the molecular weight and concentration of PVP, the type of monomer also has a significant impact on controlling the NP's surface characteristics.

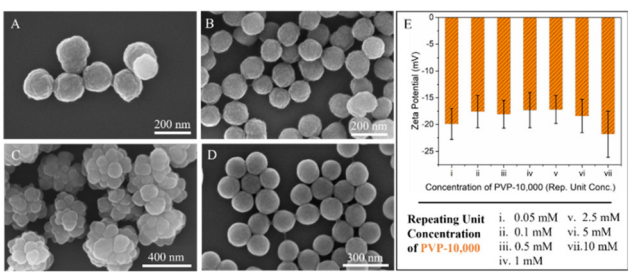

Fig. 3 PVMA NPs in the presence of PVP-10 000 (molecular weight) in the aqueous phase. SEM images of the PVMA particles synthesized in the presence of PVP-10 000 at various concentrations in the aqueous phase, where PVP acts as a surface-capping agent: (A) 10 mM (repeating unit concentration), (B) 5 mM (repeating unit concentration), (C) 1 mM (repeating unit concentration), and (D) 0.5 mM (repeating unit concentration). (E) Zeta potential measurements of PVMA NPs synthesized using PVP-10 000 in the aqueous phase at various concentrations.

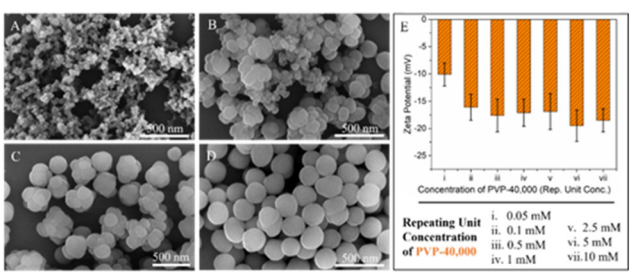

Fig. 4 PVMA NPs in the presence of PVP-40 000 (molecular weight) in the aqueous phase. SEM images of PVMA NPs synthesized in the presence of PVP-40 000 at various concentrations in the aqueousphase, where PVA acts as a surface-capping agent: (A) 10 mM (repeating unit concentration), (B) 1 mM (repeating unit concentration), (C) 0.5 mM (repeating unit concentration), and (D) 0.05 mM (repeating unit concentration). (E) Zeta potential measurements of the PVMA NPs synthesized using PVP-40 000 in the aqueous phase at various concentrations.

When PVP-40 000 at 1 mM repeating unit concentration was used in the aqueous phase during polymerization, a progressive assembling pattern in the PVMA colloidal particles was observed as shown in Fig. 4B. According to the aggregation behaviour of nanoparticles,[59] it is reasonable to assume that when the surface-capping agent concentration decreases, the growing particles prefer to minimize their surface energy as the surface is not densely covered with PVP. At 1 mM critical concentration, flower-shaped aggregates, and non-aggregated, rather 'fluffy' remaining products were observed (Fig. 4B). With the further decrease of the PVP-40 000 concentration in the aqueous phase (that is, 0.5 mM), almost all PVMA NPs were formed with a flower shape as shown in Fig. 4C. Despite the long PVP chain, hydrophobic PVMA particles aggregated and formed textured surfaces due to the low concentration. Spherical type PVMA particles were obtained using PVP-40 000 at a concentration of 0.05 mM as shown in Fig. 4D. The zeta potential of the PVMA NPs in the aqueous phase is shown in Fig. 4E.

2.1.3 Utilizing PVP-360 000 (molecular weight) in the aqueous phase. Finely textured assembled particles were obtained using 10 mM PVP-360 000 as shown in Fig. 5A. When the concentration of PVP-360 000 decreased to 5 mM repeating unit concentration, rather 'fluffy' NPs were observed (Fig. 5B). With the further decrease of the PVP-360 000 concentration (2.5 mM), non-assembled 'fluffy' NPs were observed (Fig. 5C) similar to the NPs obtained using 10 mM PVP-40 000 in Fig. 4A. No significant difference in the impact of 2.5 mM PVP-360 000 and 10 mM PVP-40 000 on the NP's shape was observed (Fig. 4A and 5C). Spherical and 'fluffy' NPs were also obtained using

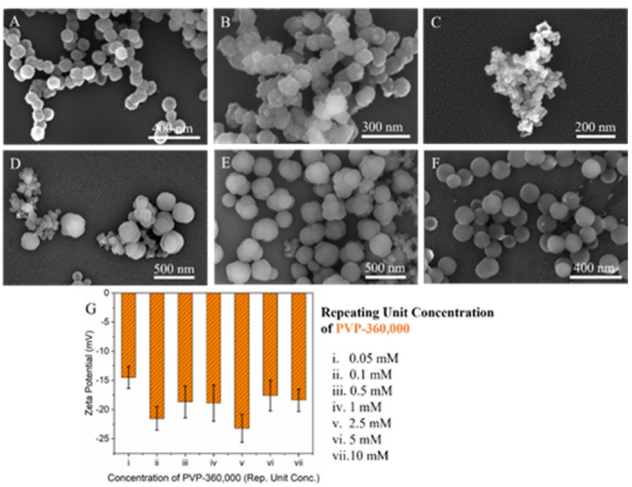

Fig. 5 PVMA NPs in the presence of PVP-360 000 (molecular weight) in the aqueous phase. SEM images of the PVMA NPs synthesized in the presence of PVP-360 000 at various concentrations in the aqueous phase, where PVP acts as a surface-capping agent: (A) 10 mM (repeating unit concentration), (B) 5 mM (repeating unit concentration), (C) 2.5 mM (repeating unit concentration), (D) 1 mM (repeating unit concentration), (E) 0.5 mM (repeating unit concentration), and (F) 0.05 mM (repeating unit concentration). (G) Zeta potential measurements of the PVMA NPs synthesized using PVP-360 000 in the aqueous phase at various concentrations.

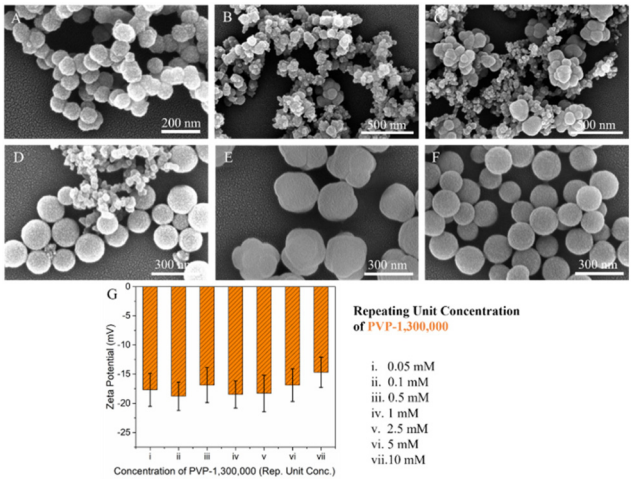

Fig. 6 PVMA NPs in the presence of PVP-1 300 000 (molecular weight) in the aqueous phase. SEM images of PVMA NPs synthesized in the presence of PVP-1 300 000 at various concentrations in the aqueous phase, where PVP acts as a surface-capping agent: (A) 10 mM (repeating unit concentration), (B) 2.5 mM (repeating unit concentration), (C) 1 mM (repeating unit concentration), (D) 0.5 mM (repeating unit concentration), (E) 0.1 mM (repeating unit concentration), and (F) 0.05 mM (repeating unit concentration). (G) Zeta potential measurements of the PVMA NPs synthesized using PVP-1 300 000 in the aqueous phase at various concentrations.

1 mM PVP-360 000 (Fig. 5D). Flower-shaped and spherical particles were obtained using 0.5 mM and 0.05 mM PVP-360 000 as shown in Fig. 5E and F, respectively. The zeta potentials of the obtained PVMA colloidal particles are shown in Fig. 5G. The minor fluctuation observed in zeta potential values may be caused by the assembling patterns of the particles.

2.1.4 Utilizing PVP-1 300 000 (molecular weight) in the aqueous phase. The surface characteristics of PVMA NPs obtained using PVP-1 300 000 are very similar to the NPs obtained using PVP-360 000 (Fig. 5 and 6). Finely textured assembled particles were obtained using 10 mM PVP-1 300 000 (Fig. 6A). In contrast, when the concentration decreased to 2.5 mM, dispersed 'fluffy' NPs were observed (Fig. 6B). Flower-shaped NPs were formed upon using 1 mM and 0.5 mM concentrations of PVP-1 300 000 (Fig. 6C and D). Moreover, larger textured assembly particles were formed at 0.1 mM concentration (Fig. 6E). When high molecular weight PVP was used at a lower concentration (0.05 mM), the polymerization created spherical type NPs with rather smooth surfaces as shown in Fig. 6F. The zeta potential of the NPs was found at around −17 mV (Fig. 6G).

A schematic illustration of the formation of PVMA colloidal particles using different molecular weights and concentrations of PVP is shown in Fig. 7. Overall, based on the molecular weight and concentration, by utilization of PVP in the aqueous phase, flower-shaped and spherical-shaped NPs were obtained.

2.2. Colloidal PVMA particles: impact of tunable molecular weights and concentrations of PSSS

PSSS is an anionic polyelectrolyte and contains a large number of sulfonate ions. Two different molecular weights of PSSS

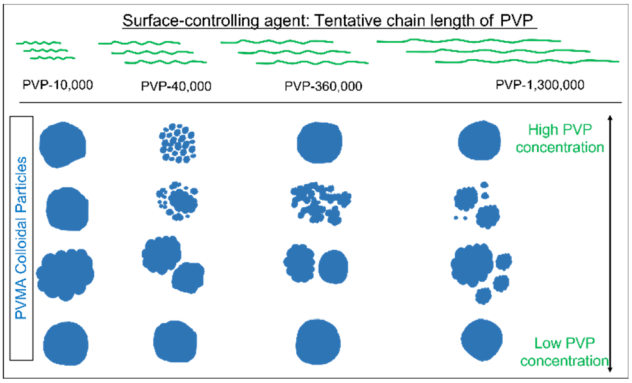

Fig. 7 Schematic overview of the formation of PVMA NPs using different molecular weights and concentrations of PVP. The PVP chain length-based estimation of the molecular weights and the schematics of the PVMA NPs obtained at higher and lower concentrations in the presence of PVP at various molecular weights.

(70 000 and 200 000) were used at six different concentrations (0.1 mM to 20 mM). The linear assembling pattern of PVMA NPs is similar to the assembling pattern of PMMA NPs.[42,43]

2.2.1 Utilizing PSSS-70 000 (molecular weight) in the aqueous phase. Here, we used PSSS-70 000 in the aqueous phase during polymerization. When 20 mM PSSS-70 000 was used in the aqueous phase, elongated spherical PVMA colloidal particles were obtained (Fig. 8A). On the other hand, elongated assembled PMMA NPs can also be obtained by using PSSS-70 000.[43] This comparison shows that not only the PSSS molecular weights but also the type of monomer are very crucial for the final NP shape. When the concentration of PSSS-70 000 decreased from 20 mM to 10 mM, 2.5 mM, and 1 mM (repeating unit concentrations), spherical PVMA NPs were obtained in all cases as shown in Fig. 8B–D. The zeta potential value is dependent on the charge and concentration of surface capping agents on the surface of polymeric nanoparticles. The zeta potential value of the PVMA NPs increased in the negative direction correlated with the increase of the anionic PSSS concentration as shown in Fig. 8E.

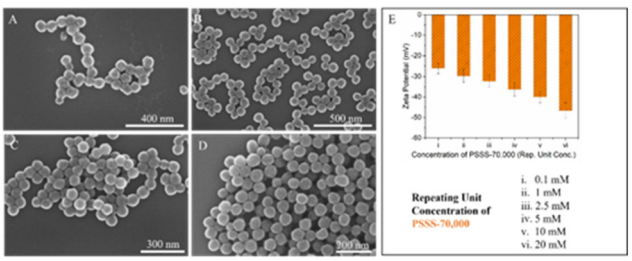

Fig. 8 PVMA NPs were obtained in the presence of PSSS-70 000 (molecular weight). SEM images of the PVMA NPs synthesized in the presence of anionic polyelectrolyte PSSS-70 000 at various concentrations in the aqueous phase, where PSSS acts as a surface-capping agent: (A) 20 mM (repeating unit concentration), (B) 10 mM (repeating unit concentration), (C) 2.5 mM (repeating unit concentration), and (D) 0.1 mM (repeating unit concentration). (E) Zeta potential measurements of PVMA NPs synthesized using PSSS-70 000 in the aqueous phase at various concentrations.

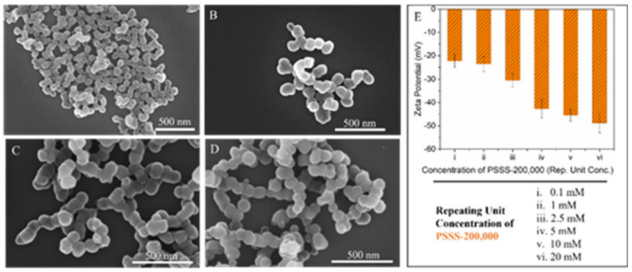

Fig. 9 PVMA NPs were obtained in the presence of PSSS-200 000 (molecular weight) in the aqueous phase. SEM images of the PVMA NPs synthesized in the presence of anionic polyelectrolyte PSSS-200 000 at various concentrations in the aqueous phase, where PSSS acts as a surface-capping agent: (A) 20 mM (repeating unit concentration), (B) 5 mM (repeating unit concentration), (C) 1 mM (repeating unit concentration), and (D) 0.1 mM (repeating unit concentration). (E) Zeta potential measurements of the PVMA NPs synthesized using PSSS-200 000 in the aqueous phase at various concentrations.

2.2.2 Utilizing PSSS-200 000 (molecular weight) in the aqueous phase. Linear direction assembled elongated spherical PVMA NPs were obtained using 20 mM (repeating unit concentration) PSSS-200 000 as shown in Fig. 9A. It is hypothesized that the PSSS chains breaking apart due to the assembling of hydrophobic entities in the aqueous solution resulted in linearly assembled PVMA nanoparticles.[43] The linear direction assembled PVMA NPs obtained using 5 mM, 1 mM, and 0.5 mM (repeating unit concentrations) PSSS-200 000 are shown in Fig. 9B, C and D, respectively. The zeta potentials of the NPs are strongly dependent on the concentration of PSSS. The zeta potential values of the NPs decreased with increasing PSSS concentration in the aqueous phase as shown in Fig. 9E.

3. Conclusions

In this work, the formation of *in situ* assembled PVMA NPs is demonstrated by using surface-capping agents, PVP and PSSS, of tunable molecular weights and concentrations *via* semi-microfluidic emulsion polymerization. The molecular weight and concentration of surface-capping agents influenced the assembling process, resulting in the formation of anisotropic PVMA NPs with various shapes. Specifically, fine textured NPs were obtained at high PVP concentrations (5 mM to 10 mM, molecular weight dependent), while flower-shaped NPs were obtained at lower concentrations (0.5 mM to 1 mM, molecular weight dependent). Reducing the concentration of PVP (0.05 mM to 0.5 mM, molecular weight dependent) resulted in the formation of spherical NPs at all molecular weights. Elongated spherical and spherical PVMA NPs were obtained using PSSS (70 000, molecular weight), while linear direction assembled elongated spherical NPs were formed using PSSS (200 000, molecular weight), regardless of the concentration. Controlling the self-assembly of soft polymeric materials is challenging in a single-step continuous polymerization. We developed a controllable microfluidic-supported method to

tune the surface properties of the PVMA NPs. New synthesis strategies are required to be explored in a wide range of polymeric systems for generating diverse structures of biocompatible and biodegradable nanoparticles useful in a broad spectrum of biological applications.

4. Experimental section

4.1 Materials and chemicals

Vinyl methacrylate (VMA) (Sigma-Aldrich, 98%), ethylene glycol dimethacrylate (EGDMA) (Sigma-Aldrich, 98%), azobisisobutyronitrile (AIBN) (Sigma-Aldrich, 98%), poly(styrene sulfonate sodium salt) (PSSS, 70 000 MW, 200 000 MW, Sigma-Aldrich), and polyvinyl pyrrolidone (PVP, 10 000 MW, 40 000 MW, 360 000 MW, 1 300 000 MW, Sigma-Aldrich) were used as received without further purification. Ultrapure water (Milli-Q) was used in all experiments.

4.2 Microfluidic-supported synthesis of PVMA NPs

In this study, a microfluidic reactor[35] was used for the formation of an emulsion of two immiscible liquid phases and conducting emulsion polymerization. The microreactor was fabricated *via* the lithography technique.[35] The microfluidic-supported emulsification of two immiscible liquids and their polymerization on the heating block outside the microfluidic reactor are shown in Fig. 1. The emulsification of both immiscible phases takes place in the microreactor, but the polymerization is completed on the heating block.

The formation of PVMA nanoparticles was performed by emulsion polymerization. Two immiscible liquid phases were prepared separately for emulsification: an aqueous phase (continuous phase) and a monomer phase (dispersed phase). The aqueous phase is composed of surface-capping agents (PSSS or PVP) with different molecular weights and concentrations. The monomer phase is composed of a mixture of vinyl methacrylate (VMA, monomer), ethylene glycol dimethacrylate (EGDMA, cross-linker), and azobisisobutyronitrile (AIBN, thermal initiator). For preparing 1 mL of monomer phase solution, 4 μg AIBN and 10 μL EGDMA were dissolved in 990 μL of VMA. For the microfluidic system, pumps from New Era Pump System Inc. were used as shown in Fig. 1. A 1200 μL min^{-1} flow rate was used for the monomer phase and an 80 μL min^{-1} flow rate was used for the aqueous phase. The emulsion was obtained by mixing two immiscible phases in a microfluidic platform and the polymerization took place in a small vial on the heating block at 95 °C for 20 min (Fig. 1). The PVMA NPs were washed with ultrapure water through two cycles of centrifugation (11 000 RPM, 12 minutes) using a Thermo Fisher centrifuge. The purified PVMA NPs were characterized using scanning electron microscopy (SEM) and a zetasizer.

4.3 Characterization of PVMA NPs

4.3.1 Scanning electron microscopy (SEM) characterization. 10 μL of PVMA nanoparticles were diluted with ultrapure water to 100 μL (dilution) before SEM measurements. A silicon chip (made from a small 1 cm × 1 cm piece of silicon wafer using a micro-cutter) was used for preparing the samples for characterization. The sample on the silicon chip was covered with gold using a Leica EM ACE600 Coater (thickness: 2.7 nm). An FEI Helios Nanolab 660 FIB-SEM was used for the characterization of PVMA nanoparticles. Images were taken at 5 kV voltage and 25 pA current at multiple magnifications.

4.3.2 Zeta potential measurements. The zeta potential of PVMA nanoparticles was measured using a Malvern Zetasizer instrument (Zetasizer Nano Series: Nano ZS). Initially, the centrifuged particles were re-dispersed in ultrapure water. 50 μL of nanoparticle dispersion was diluted to 1 mL using ultra-pure water. Malvern DTS1070 cells were used for zeta potential measurements.

Author contributions

D.M.E. directed the project; N.R.V. designed the experiments; F.K., J.X., K.L., K.M., and L.S.P. assisted in the experimental setup and synthesis of colloidal polymer nanoparticles; J.X., C. C., T.M., and V.B. assisted in the purification and characterization of polymer nanoparticles; F.K. and L.S.P. assisted in SEM imaging; J.X., G.S., A.A., S.A., L.S.P., K.L., and F.K. assisted in zeta potential measurements; P.M. and S.K. performed data interpretation and fruitful discussions during the preparation of the manuscript; and D.M.E., S.K., and N.R.V. co-wrote the manuscript with inputs from all co-authors.

Data availability

All data used in this report have been included in the paper.

Conflicts of interest

There are no conflicts to declare.

Acknowledgements

This material is based upon work partially supported by the National Science Foundation Faculty Early Career Development Program (NSF-CAREER 1752475) and the U.S. Department of Energy, Office of Science, Office of Basic Energy Sciences (DOE DE-SC0018142). Equipment support is partially provided by the National Science Foundation Major Research Instrumentation Program (NSF-MRI 1531859). Support is partially provided by the National Science Foundation NSF-CREST Center for Interface Design and Engineered Assembly of Low Dimensional Systems (IDEALS), NSF grant number NSF-CREST HRD-1547830. This work was performed at the Center for Discovery and Innovation of The City College of New York and the Advanced Science Research Center Imaging Facility of The City University of New York. The authors thank the PSC-CUNY Research Award Program for its support.

References

1 S. Haddadi, M. Skepö, P. Jannasch, S. Manner and J. Forsman, *J. Colloid Interface Sci.*, 2021, **581**, 669–681.
2 M. J. Monteiro and M. F. Cunningham, *Biomacromolecules*, 2020, **21**, 4377–4378.
3 R. M. Fitch, *Br. Polym. J.*, 1973, **5**, 467–483.
4 R. Deng, L. Zheng, X. Mao, B. Li and J. Zhu, *Small*, 2021, **17**, 2006132.
5 J. L. Ortega-Vinuesa, A. Martín-Rodríguez and R. Hidalgo-Álvarez, *J. Colloid Interface Sci.*, 1996, **184**, 259–267.
6 F. Tiarks, K. Landfester and M. Antonietti, *Langmuir*, 2001, **17**, 908–918.
7 A. Musyanovych and K. Landfester, *Macromol. Biosci.*, 2014, **14**, 458–477.
8 E. W. Durbin and G. A. Buxton, *Soft Matter*, 2010, **6**, 762–767.
9 K. Loomis, K. McNeeley and R. V. Bellamkonda, *Soft Matter*, 2011, **7**, 839–856.
10 M. Elsabahy and K. L. Wooley, *Chem. Soc. Rev.*, 2012, **41**, 2545–2561.
11 W. Li, L. Zhang, X. Ge, B. Xu, W. Zhang, L. Qu, C.-H. Choi, J. Xu, A. Zhang, H. Lee and D. A. Weitz, *Chem. Soc. Rev.*, 2018, **47**, 5646–5683.
12 S. Jiang, A. Van Dyk, A. Maurice, J. Bohling, D. Fasano and S. Brownell, *Chem. Soc. Rev.*, 2017, **46**, 3792–3807.
13 T. Repenko, A. Rix, S. Ludwanowski, D. Go, F. Kiessling, W. Lederle and A. J. C. Kuehne, *Nat. Commun.*, 2017, **8**, 470.
14 M. Elsabahy, G. S. Heo, S.-M. Lim, G. Sun and K. L. Wooley, *Chem. Rev.*, 2015, **115**, 10967–11011.
15 S. Liu, R. Deng, W. Li and J. Zhu, *Adv. Funct. Mater.*, 2012, **22**, 1692–1697.
16 M. P. Robin and R. K. O'Reilly, *Polym. Int.*, 2015, **64**, 174–182.
17 K. Kempe, R. A. Wylie, M. D. Dimitriou, H. Tran, R. Hoogenboom, U. S. Schubert, C. J. Hawker, L. M. Campos and L. A. Connal, *J. Polym. Sci., Part A: Polym. Chem.*, 2016, **54**, 750–757.
18 M. Szczęch and K. Szczepanowicz, *Nanomaterials*, 2020, **10**, 496.
19 W. Wichaita, Y.-G. Kim, P. Tangboriboonrat and H. Thérien-Aubin, *Polym. Chem.*, 2020, **11**, 2119–2128.
20 M. A. C. Stuart, W. T. S. Huck, J. Genzer, M. Muller, C. Ober, M. Stamm, G. B. Sukhorukov, I. Szleifer, V. V. Tsukruk, M. Urban, F. Winnik, S. Zauscher, I. Luzinov and S. Minko, *Nat. Mater.*, 2010, **9**, 101–113.
21 A. Lendlein and V. P. Shastri, *Adv. Mater.*, 2010, **22**, 3344–3347.
22 S. Mura, J. Nicolas and P. Couvreur, *Nat. Mater.*, 2013, **12**, 991–1003.
23 X. Liu, Y. Yang and M. W. Urban, *Macromol. Rapid Commun.*, 2017, **38**, 1700030.
24 N. R. Visaveliya, C. W. Leishman, K. Ng, N. Yehya, N. Tobar, D. M. Eisele and J. M. Köhler, *Adv. Mater. Interfaces*, 2017, **4**, 1700929.
25 M. Božič, T. Elschner, D. Tkaučič, M. Bračič, S. Hribernik, K. S. Kleinschek and R. Kargl, *Cellulose*, 2018, **25**, 6901–6922.
26 T. Urbaniak and W. Musiał, *Nanomaterials*, 2019, **9**, 1240.
27 L. Yu, N. Zhang, N.-N. Zhang, Q. Gu, Y. Xue, Y.-X. Wang, C.-L. Han, K. Liu, Z.-Y. Sun, H.-J. Qian and Z.-Y. Lu, *J. Phys. Chem. Lett.*, 2021, **12**, 7100–7105.
28 C. S. Chern, *Prog. Polym. Sci.*, 2006, **31**, 443–486.
29 P. A. Lovell and F. J. Schork, *Biomacromolecules*, 2020, **21**, 4396–4441.
30 N. Visaveliya and J. M. Köhler, *Langmuir*, 2014, **30**, 12180–12189.
31 A. Gharieh, S. Khoee and A. R. Mahdavian, *Adv. Colloid Interface Sci.*, 2019, **269**, 152–186.
32 H. Heinz, C. Pramanik, O. Heinz, Y. Ding, R. K. Mishra, D. Marchon, R. J. Flatt, I. Estrela-Lopis, J. Llop, S. Moya and R. F. Ziolo, *Surf. Sci. Rep.*, 2017, **72**, 1–58.
33 J. P. Rao and K. E. Geckeler, *Prog. Polym. Sci.*, 2011, **36**, 887–913.
34 T. Al Najjar, N. K. Allam and E. N. El Sawy, *Nanoscale Adv.*, 2021, **3**, 5626–5635.
35 J. M. Koehler, F. Moeller, S. Schneider, P. M. Guenther, A. Albrecht and G. A. Gross, *Chem. Eng. J.*, 2011, **167**, 688–693.
36 S. Javadian and J. Kakemam, *J. Mol. Liq.*, 2017, **242**, 115–128.
37 E. A. Appel, M. W. Tibbitt, M. J. Webber, B. A. Mattix, O. Veiseh and R. Langer, *Nat. Commun.*, 2015, **6**, 6295.
38 E. L. Correia, N. Brown and S. Razavi, *Nanomaterials*, 2021, **11**, 374.
39 N. J. Alvarez, S. L. Anna, T. Saigal, R. D. Tilton and L. M. Walker, *Langmuir*, 2012, **28**, 8052–8063.
40 M. Urban, B. Freisinger, O. Ghazy, R. Staff, K. Landfester, D. Crespy and A. Musyanovych, *Macromolecules*, 2014, **47**, 7194–7199.
41 H. Zou and S. Zhai, *Polym. Chem.*, 2020, **11**, 3370–3392.
42 N. Visaveliya and J. M. Kohler, *ACS Appl. Mater. Interfaces*, 2014, **6**, 11254–11264.
43 N. Visaveliya and J. M. Kohler, *Macromol. Chem. Phys.*, 2015, **216**, 1212–1219.
44 J. A. Champion and S. Mitragotri, *Proc. Natl. Acad. Sci. U. S. A.*, 2006, **103**, 4930–4934.
45 O. C. Farokhzad and R. Langer, *ACS Nano*, 2009, **3**, 16–20.
46 H. Minami, K. Yoshida and M. Okubo, *Macromol. Rapid Commun.*, 2008, **29**, 567–572.
47 S. Shen, E. D. Sudol and M. S. Elaasser, *J. Polym. Sci., Part A: Polym. Chem.*, 1993, **31**, 1393–1402.
48 T. H. Yang, Y. F. Shi, A. Janssen and Y. N. Xia, *Angew. Chem., Int. Ed.*, 2020, **59**, 15378–15401.
49 N. R. Visaveliya, S. Kelestemur, F. Khatoon, J. Xu, K. Leo, L. St. Peter, C. Chan, T. Mikhailova, V. Bexheti, A. Kapadia, P. Maity, W. P. Carbery, K. Ng and D. M. Eisele, *Polym. Chem.*, 2022, **13**, 4625–4633.
50 J. Nicolas, Y. Guillaneuf, C. Lefay, D. Bertin, D. Gigmes and B. Charleux, *Prog. Polym. Sci.*, 2013, **38**, 63–235.

51 W. A. Braunecker and K. Matyjaszewski, *Prog. Polym. Sci.*, 2007, **32**, 93–146.
52 S. Perrier, *Macromolecules*, 2017, **50**, 7433–7447.
53 S. Harrisson, X. Liu, J.-N. Ollagnier, O. Coutelier, J.-D. Marty and M. Destarac, *Polymers*, 2014, **6**, 1437–1488.
54 R. Karnik, F. Gu, P. Basto, C. Cannizzaro, L. Dean, W. Kyei-Manu, R. Langer and O. C. Farokhzad, *Nano Lett.*, 2008, **8**, 2906–2912.
55 C. N. Baroud, F. Gallaire and R. Dangla, *Lab Chip*, 2010, **10**, 2032–2045.
56 C. A. Serra and Z. Q. Chang, *Chem. Eng. Technol.*, 2008, **31**, 1099–1115.
57 J. M. Kohler, S. N. Li and A. Knauer, *Chem. Eng. Technol.*, 2013, **36**, 887–899.
58 Z. Hua, J. R. Jones, M. Thomas, M. C. Arno, A. Souslov, T. R. Wilks and R. K. O'Reilly, *Nat. Commun.*, 2019, **10**, 5406.
59 S. Shrestha, B. Wang and P. Dutta, *Adv. Colloid Interface Sci.*, 2020, **279**, 102162.
60 B. J. Liu, Y. J. Wang, M. Y. Zhang and H. X. Zhang, *Polymers-Basel*, 2016, **8**(55).
61 G. Oster and E. H. Immergut, *J. Am. Chem. Soc.*, 1954, **76**, 1393–1396.
62 M. Yamashina, Y. Sei, M. Akita and M. Yoshizawa, *Nat. Commun.*, 2014, **5**, 4662.